RESEARCH ARTICLE

Underwater Acoustic DOA Estimation of Incoherent Signal Based on Improved GA-MUSIC

CHAOFENG LAN[1], HUAN CHEN[2], LEI ZHANG[3], RUI GUO[1], CHUANG HAN[1], AND DAJUN LUO[1]

[1]School of Measurement and Communication Engineering, Harbin University of Science and Technology, Harbin 150080, China
[2]China Ship Development and Design Center, Wuhan 430064, China
[3]Beidahuang Industry Group General Hospital, Harbin 150088, China

Corresponding authors: Lei Zhang (happyzhang68@126.com), Rui Guo (guo29rui@163.com), and Dajun Luo (760905927@qq.com)

ABSTRACT The problem of poor real-time capability, a large number of traversals and the long operation time of the MUSIC algorithm bring great difficulties to the application of DOA estimation. For the above problems, this paper fuses MUSIC algorithm and genetic algorithm and proposes an improved genetic MUSIC algorithm (GA-MUSIC). Also, improvement strategies are proposed for the three operators of selection, crossover, and variation of the genetic algorithm. The GA-MUSIC was simulated for DOA estimation to verify the effectiveness of this algorithm. The research shows that the GA-MUSIC proposed in this paper has the best operational performance at different precisions and SNRs. This algorithm can effectively reduce the iterative computation of the algorithm with better real-time performance, and the search success rate is above 95% while ensuring accuracy. Furthermore, this paper corroborates that the proposed improved genetic MUSIC algorithm can achieve better performance in single signals and incoherent multi-signal sources. It can be seen that the algorithm in this paper can effectively solve the problems of low success rates of DOA estimation searches and poor real-time performance and has a significant reference value for practical engineering applications.

INDEX TERMS DOA estimation, MUSIC algorithm, genetic algorithm, GA-MUSIC, real-time.

I. INTRODUCTION

DOA estimation is an essential technique in the research direction of array signal processing, essentially determining target orientation information using spatial spectrum estimation [1], [2], [3]. With the continuous development of science and technology as well as the increasing maturity of hardware and software equipment, high-resolution and high-precision DOA estimation technology has been successfully applied in various applications, including wireless communications, rock cave mining, underground survey, space exploration, and industrial and military fields [4], [5], [6], [7]. However, measurement accuracy is not ideal in underwater acoustic engineering, mainly because the complex and changeable marine underwater environment

The associate editor coordinating the review of this manuscript and approving it for publication was Chengpeng Hao.

dramatically affects the reception of signals. Moreover, most high-resolution algorithms have the defects of high requirements on the signal-to-noise ratio (SNR) and poor real-time performance caused by a large amount of calculation. Therefore, it is significant for practical engineering to study a DOA estimation parameter algorithm that can solve the above problems.

To the complexity of the underwater environment, the array method is usually selected to send and receive signals in the orientation estimation of underwater targets. The primary technical means of underwater target DOA estimation are Beam-Forming, Compressive Sensing and Subspace Classification [8]. In recent years, due to the higher resolution and the need for a single measurement snapshot, making Compressive Sensing known as a popular research method for DOA estimation, such as compressive DOA [9], [10], [11]. However, this technique is constrained by a fixed grid,

and in response, off-grid or gridless methods emerged. Some methods exploit the sparsity in the atomic parametrization of the measurements [12], [13], [14]. In practice, sparse representation methods suffer from a high computational complexity. In contrast, MUSIC methods are less computational complexity [15], [16]. With high resolution and precision, Multiple Signal Classification (MUSIC) algorithm is a subspace classification method and realizes super-resolution channel parameter estimation, which R.O. Schmidt proposed in 1979. It can search for multiple target sources and maintain the accuracy of bearing estimation. Furthermore, this algorithm is a significant turning point in the development of bearing estimation algorithms, which truly realize super-resolution channel parameter estimation [17], [18], [19], [20]. However, MUSIC algorithm has high requirements for the number of snapshots in the detection array and many complex matrix operations. Moreover, accurate DOA estimation cannot be performed for coherent signals, resulting in poor real-time performance [21], [22], [23], [24]. To solve the problems of search success rate, computing time, and real-time for non-coherent multi-signal source DOA estimation in practical engineering applications, scholars have proposed improved MUSIC algorithms for coherent signal DOA estimation, such as the Rotation Invariant Method [25], the Maximum Likelihood Estimation Method [26], a Joint Processing-MUSIC Algorithm [27], and improved MUSIC Pseudo-Likelihood [28]. Besides, to solve the problem of enormous computation amounts in spectral peak search with the development of technology, some scholars have proposed that the subspace rotation invariance of sound signals be introduced into azimuth estimation. The disadvantage of this method is that the accuracy and resolution of orientation estimation are lower than those of the MUSIC algorithm. In addition, various subspace DOA estimation algorithms have emerged, for example, the augmented subspace (AS) MUSIC method proposed in [29] and the weighted subspace fitting (WSF) method proposed in [30]. These algorithms have been improved from different perspectives.

The theory of genetics was born based on the differences in characteristics exhibited by organisms during the evolutionary process. Genetic algorithms can explore several points in the search space simultaneously, thus reducing the chance of convergence to a local optimum. Moreover, it can reorganize structural information to locate new points in the search space with the expected performance improvements. In particular, it does not require the assumption of a differentiable or continuous search space and also allows several iterations on each received data. Reference [31] proposed an iterative MUSIC search technique incorporating a genetic algorithm (GA) to select the initial search angle resulting in fast convergence and high estimation accuracy of DOA estimation.

Such approaches, however have failed to address significantly increasing the iterative computation and fast positioning of algorithms. In this paper, the traditional MUSIC algorithm is improved by taking advantage of the genetic algorithm's parallelism, global optimization search, and simplicity. Compared with traditional MUSIC algorithms, this algorithm can reduce the number of complex traversals and computing time. In addition, this paper also proposes improvement strategies for the three operators of selection, crossover, and variation of the genetic algorithm, improve the performance of the global search of genetic algorithms and eliminate the immature convergence phenomenon. Simulation results demonstrate that the proposed method improves the search success rate, reduces iterative computation, improves accuracy, and enhances real-time performance.

The remainder of this paper is as follows: Section II introduces the derivation process of the conventional MUSIC algorithm and the design flow of the improved method. Section III performs simulation experiments and a comparative analysis of the results. Section IV conducts experimental tests to verify the feasibility of the improved algorithm in engineering. Section V concludes the paper.

II. METHODS
A. MUSIC ALGORITHM
The MUSIC algorithm decomposes the covariance matrix of an array of output data. The decomposition yields a signal subspace corresponding to the signal components and a noise subspace orthogonal to the signal components. And then use the orthogonality of the signal and noise spaces to estimate the signal parameters, introducing the concept of vector space into the field of spatial spectrum estimation. The derivation process is as follows.

According to the relative position of array elements in a uniform linear array, the mathematical model of the received far-field narrowband signal can be expressed as:

$$X(t) = A(\theta)S(t) + N(t) \tag{1}$$

where $X(t)$ is the output matrix of the array, $S(t)$ is the matrix of the incoming signal, $N(t)$ is the vector matrix of Gaussian white noise, and $A(\theta)$ is the direction vector matrix of vector hydrophone. Assuming there are N far-field sound sources and M elements in the uniform linear array.

The reception performance of the uniform line array is optimal when the array element spacing is a half wavelength. At this time, the array guidance vector can be expressed as:

$$\alpha(\theta) = \begin{bmatrix} 1 \\ \exp(j\pi d) \\ \vdots \\ \exp(j(M-1)\pi d) \end{bmatrix}^T \tag{2}$$

where M is the number of array elements, T stands for transpose.

The target signal is received by a detection array composed of vector hydrophones, and the signal space covariance

matrix is calculated, which can be expressed as:

$$\begin{aligned} R &= [XX^H] \\ &= AE[SS^H]A^H + \sigma^2 I \\ &= AR_S A^H + \sigma^2 I \end{aligned} \qquad (3)$$

where X^H is conjugate transpose of the matrix. Since the signal subspace is orthogonal to the noise subspace, R can be decomposed into two parts that intersect independently with the subspace. $AR_S A^H$ denotes the signal part, R_S denotes the covariance matrix of the signal, I is the identity matrix.

The eigenvalue decomposition of R can be expressed as:

$$R = U\Sigma U^H \qquad (4)$$

where U is the Characteristic Vectors matrix, U^H is the transposed characteristic vector matrix. Moreover, Σ is the diagonal matrix consisting of all eigenvalues. Then Σ can be expressed as:

$$\Sigma = \begin{bmatrix} \lambda_1 & & & \\ & \lambda_2 & & \\ & & \ddots & \\ & & & \lambda_M \end{bmatrix} \qquad (5)$$

in the formula (5), the eigenvalues in the diagonal matrix should satisfy the following conditions:

$$\lambda_1 \geq \lambda_2 \geq \cdots \geq \lambda_N > \lambda_{N+1} = \cdots = \lambda_M = \sigma^2 \qquad (6)$$

where M is the number of elements in the uniform linear array; N is the number of far-field sound sources.

Now construct two diagonal matrices as follows:

$$\Sigma_S = \begin{bmatrix} \lambda_1 & & & \\ & \lambda_2 & & \\ & & \ddots & \\ & & & \lambda_N \end{bmatrix}, \ \Sigma_N = \begin{bmatrix} \lambda_{N+1} & & & \\ & \lambda_{N+2} & & \\ & & \ddots & \\ & & & \lambda_M \end{bmatrix} \qquad (7)$$

where Σ_S is a diagonal matrix composed of large parts of eigenvalues, Σ_N is a diagonal matrix of the remaining eigenvalues.

When the spatial noise is white noise, then it can be expressed as:

$$\Sigma_N = \sigma^2 I_{(M-N)\cdot(M-N)} \qquad (8)$$

In addition, the characteristic vector matrix can also be divided into two parts: one part is the signal subspace $US = [e_1, e_2, \ldots, e_n]$ corresponding to Σ_S; the other part is the noise subspace $UN = [e_{n+1}, e_{n+2}, \ldots, e_M]$ corresponding to Σ_N. The covariance matrix can be expressed as:

$$\begin{aligned} R &= \sum_{i=1}^{N} \lambda_i e_i e_i^H + \sum_{j=N+1}^{M} \lambda_j e_j e_j^H \\ &= U_S \Sigma_S U_S^H + U_N \Sigma_N U_N^H \end{aligned} \qquad (9)$$

where H is the conjugate matrix.

The independent orthogonal characteristics of the signal and noise subspaces in the MUSIC algorithm can be expressed as:

$$\alpha^H(\theta)U_N = 0 \qquad (10)$$

equation (10) is the most important step in the derivation of the basic principles of the MUSIC algorithm. In engineering applications, the received signal data are of finite length. So the maximum likelihood estimation of the covariance matrix can be expressed as:

$$\widehat{R} = \frac{1}{L} \sum_{i=1}^{L} X(i)X(i)^H \qquad (11)$$

the noise subspace feature vector matrix $\widehat{U}_N$ can be obtained by decomposing $\widehat{R}$.

There are many interference factors in underwater target detection. So, the signal and noise subspaces of engineering data measurements are not orthogonal in most cases. The minimum optimization search method is usually used to obtain the position of underwater targets. The angle estimate can be expressed as:

$$\theta_{MUSIC} = \arg\min_\theta \alpha^H(\theta)\widehat{U}_N \widehat{U}_N^H \alpha(\theta) \qquad (12)$$

From Equation (12), the spectral estimate of the MUSIC algorithm is obtained, expressed as:

$$P_{\theta(MUSIC)} = \frac{1}{\alpha^H(\theta)\widehat{U}_N \widehat{U}_N^H \alpha(\theta)} \qquad (13)$$

according to equation (13), the spectral peak search is carried out in the range of target signal parameters. Calculate the azimuth angle corresponding to the global extreme point. Determine the incident direction of the received signal, then determine the target orientation.

B. GENETIC ALGORITHM (GA)

The Genetic algorithm is an optimization method that mimics the evolutionary process of organisms and seeks the optimal solution by searching. The process of GA-MUSIC algorithm is as follows:

1) SELECTION

The selection is based on the fitness value of the coding string as a judgment criterion to determine whether the coding string can be copied to the next generation. The expectation of the number of individuals being replicated in the population is expressed as follows:

$$nr = Z \cdot f(si)/\sum_{j=1}^{Z} f(sj) \qquad (14)$$

where $f(si)$ is the fitness value of the si individual and Z is the population size. To achieve the replication operation, the total

fitness value of the population needs to be obtained, which can be expressed as:

$$F = \sum_{j=1}^{Z} f(sj) \tag{15}$$

From the above equation, the probability of all individuals being replicated can be obtained and can be expressed as:

$$ps(si) = f(si)/F \tag{16}$$

then the cumulative probability of individual si can be expressed as:

$$qi = \sum_{j=1}^{i} sj \tag{17}$$

The selection operator adopts the optimal solution strategy of roulette bet combination as follows:

1. Generate a random number r, and the range of values of r is [0,1];

2. If $qi - 1 \leq r \leq qi$, individual si is selected as the parent individual for the next operation. The higher the fitness value of an individual, the greater the chance of becoming a parent, and the lower the fitness value, the easier it is to be eliminated, which fully reflects the evolutionary theory of "survival of the fittest" in nature, i.e., the best individuals will be reproduced and the inferior ones will be eliminated.

2) CROSSOVER
The crossover operator uses probabilistic crossover or multi-point crossover with the difference in fitness of contemporary individuals, and the crossover operation can be expressed as follows:

$$\begin{aligned} A &= (a1a2a3a4|a5a6a7 \cdots al) \\ B &= (b1b2b3b4|b5b6b7 \cdots bl) \end{aligned} \text{parents}$$
$$\Rightarrow\Rightarrow\Rightarrow$$
$$\begin{aligned} A &= (a1a2a3a4|b5b6b7 \cdots bl) \\ B &= (b1b2b3b4|a5a6a7 \cdots al) \end{aligned} \text{children} \tag{18}$$

3) VARIATION
The variation operator performs a balanced variation in the proportion of genetic values of individuals in the population according to the variability of the contemporary population, which maintains the population diversity and improves the local search ability of the algorithm.

$$\begin{aligned} A &= (a102a3a4|a516a7 \cdots al) \\ B &= (b112b3b4|b506b7 \cdots bl) \end{aligned} \text{parents}$$
$$\Rightarrow\Rightarrow\Rightarrow$$
$$\begin{aligned} A &= (a112a3a4|b506b7 \cdots bl) \\ B &= (b102b3b4|a516a7 \cdots al) \end{aligned} \text{children} \tag{19}$$

C. IMPROVED GENETIC ALGORITHM
In this paper, the optimization improvement strategy of the genetic algorithm for the operator.

1) IMPROVEMENT OF THE SELECTION OPERATOR
Ranking the individuals according to their fitness size from largest to smallest, define the probability that the individual V_i corresponding to the serial number i is selected as p_i, where the probability p_i can be expressed as:

$$p_i = \frac{1}{Popsize} + \alpha(gen)\frac{Popsize + 1 - 2i}{Popsize(popsize + 1)} \tag{20}$$

In Eq. (20), $Popsize$ is the population size, and $\alpha(gen)$ is a function of the generation function gen which mainly determines the size of the difference in the probability of selection of adjacent individuals in the population. $\alpha(gen)$ is a segmented discontinuity function, which can be expressed as:

$$\alpha(gen) = \begin{cases} 0.3 & 0 \leq gen < (MaxGen/20) \\ 0.5 & (MaxGen/20) \leq gen < (MaxGen/4) \\ 0.7 & gen \geq (MaxGen/4) \end{cases} \tag{21}$$

In Eq. (21), $MaxGen$ is the maximum number of evolutionary generations. After the probability of selection of individuals in the population is determined, the probability of selection is determined by combining the roulette wheel with the roulette wheel, i.e., by dividing the region on the roulette wheel according to the probability, and when the roulette wheel is rotated, the selection is made by throwing darts, and the individuals in the region where the darts are located are the selected individuals.

2) IMPROVEMENT OF THE SELECTION OPERATOR
In this paper, we compare the similarity of the binary codes before the chromosome crossover. The similarity degree w can be expressed as:

$$w = \sum_{i=1}^{n} \left(x_i^{(1)} - x_i^{(2)}\right)^2 \tag{22}$$

In Eq. (22), $x_i^{(1)}$, $x_i^{(2)}$ are the ith position of the two paired individuals, respectively, and n is the length of the individual code. If w is greater than a very small positive number ε, the chromosomes of these two individuals can cross over; if not, they are considered close relatives, and another individual is reselected from the population to cross over. In Eq. (22), are the digits of the two paired individuals, respectively, and are the individual coding lengths. If the chromosomes of these two individuals are greater than a very small positive number, they can cross over; if not, they are considered inbred, and a new individual is selected from the population to cross over.

3) IMPROVEMENT OF THE VARIATION OPERATOR
According to the pattern theory, the main cause of immature convergence in genetic algorithms is the loss of pattern, i.e., the premature loss of certain gene values in the genetic code, then balancing the proportion of each gene value in the population and reducing the chance of losing gene values can

overcome immature convergence to some extent. The concept of orthogonality and gene compensation inspires them. An orthogonal variation operator is used in this paper for gene equalization. The orthogonal variation operator consists of two main operations: a heterogeneous operation and a take inverse operation.

The binary code string $S_1 = a_1, a_2, \cdots, a_i, \cdots, a_L$, $S_2 = b_1, b_2, \cdots, b_i, \cdots, b_L$, where $a_i, b_i \in \{0, 1\}$, of chromosome code length L is the new code string S'_1, $S'_1 = c_1, c_2, \cdots, c_i, \cdots, c_L$, where $c_i = a_i \oplus b_i$. The new chromosome encoding string S'_1 is inverse, and the new chromosome encoding is $S'_2 = d_1, d_2, \cdots, d_i, \cdots, d_L$, where d_i is the value of c_i after inversion, i.e., "0" $\rightarrow$ "1", "1" $\rightarrow$ "0".

After the orthogonal variation operator, the population comprises pairs of individuals with mutually orthogonal chromosome codes. The process of the orthogonal variation operator is as follows: firstly, two individuals in the population are selected, and the gene values on the same locus of the binary code of these two individuals are hetero-orthogonalized to obtain a new chromosome code; secondly, the new chromosome code produced by the hetero-orthogonalization operation is inverted to obtain another new chromosome. From the above operations, a chromosome pair with an orthologous relationship is obtained, and the chromosome pair is used as the offspring to replace the original two paternal individuals. Thus, the population after the orthogonal variation operator is composed of chromosome pairs with orthogonal relationships, and the proportion of genes with "0" and "1" in each locus reaches a maximum of 50%, balancing the genes with "0" and "1" in each locus. This balanced the proportion of "0" and "1" in each locus, prevented the absence of gene values, and increased the diversity of the population to some extent. Although the orthogonal variation operator strengthens the global nature of the variation operation of the genetic algorithm and expands the search range, the disadvantage of the poor local search ability of this variation operator reduces the convergence speed of the algorithm, and it is even more difficult to converge to the optimal solution.

In order to improve the convergence of the genetic algorithm and the local search ability, the variational operation is performed by using multi-locus variation in the middle and late stages of the genetic algorithm to find the optimal solution. The orthogonal variation operator at the early stage of evolution can increase the proportion of overall gene values in the population, which is conducive to the global scope of the search for the optimal, thus reducing the chance of losing the gene values of the multi-locus variation operator with smaller variation probability at the middle and late stages of evolution, improving the local search ability of the algorithm, and can accelerate the convergence speed of the algorithm.

D. IMPROVED GA-MUSIC(GA) ALGORITHM

The massive computational volume of spectral peak search can lead to a certain degree of limitation in the real-time performance of the MUSIC algorithm. Therefore, this paper proposes a method that combines genetic and MUSIC algorithms to search for spectral peaks. The algorithm can use the genetic algorithm and population optimization operators to solve the problem of immature convergence and the defect of having fallen into local optimal solutions in the MUSIC algorithm. The specific design steps are as follows:

1) Establish a suitable array model. Find the covariance matrix of the received data array, make the eigenvalue decomposition, and get the MUSIC spectral estimation expression according to the MUSIC algorithm, which is the fitness function;
2) Determine the initialized population. Initialization of the parameters of the genetic algorithm: including the digital coding method, population size (*Popsize*), selection strategy, crossover probability (P_c), and mutation probability (P_m);
3) To assess each individual's fitness in the contemporary population and calculate the fitness size;
4) Judging the accuracy of target positioning and individual advantages due to fitness size;
5) Constructing the next-generation population through selection, crossover, and mutation operations;
6) Judging whether the current population meets the preset stopping conditions. The judgment is based on the fact that there is almost no difference between the recent iteration result and the last iteration result or that the current iteration number reaches the set maximum iteration number. Otherwise, repeat steps (4) and (5);
7) When the condition (6) is satisfied, the iteration stops, and the individual optimal solution is output. The incidence angle of the underwater target is obtained from the output judged by the fitness function. The flow chart of the GA-MUSIC is shown in Figure 1.

III. SIMULATION RESULTS AND ANALYSIS
In this section, the performance of the DOA estimation of the proposed GA-MUSIC is well investigated.

A. DOA ESTIMATION FOR SINGLE SIGNAL SOURCES
This part shows the spectral peak search of the GA-MUSIC for a single sound source at different SNRs. Simulation parameter setting: hydrophone receiving array is a five-element uniform linear array, where array element spacing $d = 25$cm, frequency of sound source $f_c = 3$kHz, the number of snapshots $SNAP$=2048, the angular range of search is $-100° \leq \theta \leq 100°$; population size $Popsize = 90$, crossover probability $P_c = 0.7$, mutation probability $P_m = 0.07$, parameter $\gamma = 0.1$, phased adjustment parameter $n = 10$, code length $L = 14$, maximum generation $MaxGen = 200$; added noise is Gaussian white noise, incidence angle is 20°, 28°, 32° and −35°. Set four SNRs of −10dB, −5dB, 0dB and 10dB. The tests under four incident angles and four working conditions are called Mode 1, Mode 2, Mode 3, and Mode 4 respectively. The spectral peak search results are shown in Figure 2.
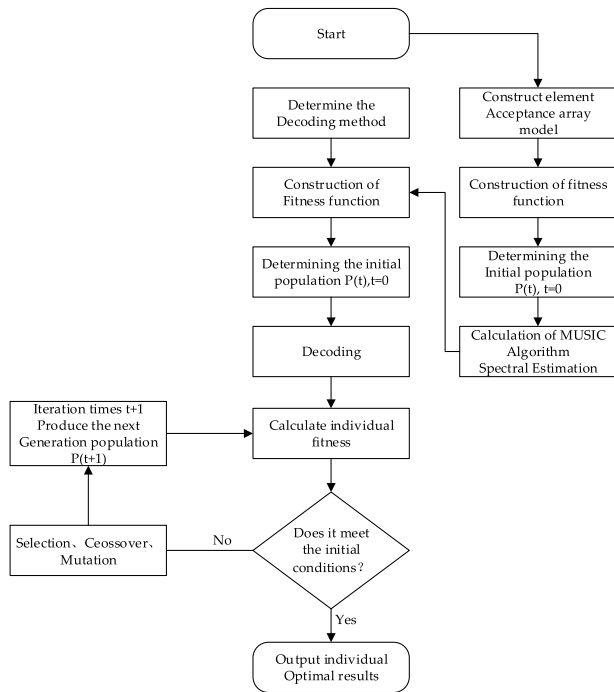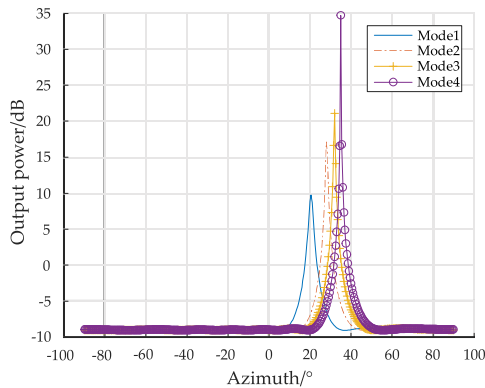
FIGURE 1. GA-MUSIC flow chart.

FIGURE 2. Time spectrum peak diagram with different SNRs.

The beam width can be used to describe the search accuracy. From Figure 2, when $SNR = -10dB$, the beam width is the largest, the search accuracy is the lowest. The error is within 3°, in line with the actual engineering application standard error. When SNR is -5 dB, the beam width is less than -10dB. When SNR is 0dB and 10dB, there is almost no interference peak, which can accurately determine the position of the target peak. At this time, the beam width is the smallest and has good search performance.

B. DOA ESTIMATION FOR MULTIPLE SOURCES

This section shows two sets of simulations to demonstrate the spatial spectrum search performance of the GA-MUSIC under multiple signal sources.

1) TWO SIGNAL SOURCES

Resolution is defined as: Let θ_1 and θ_2 separately determine the angle of the two target incident signals. According
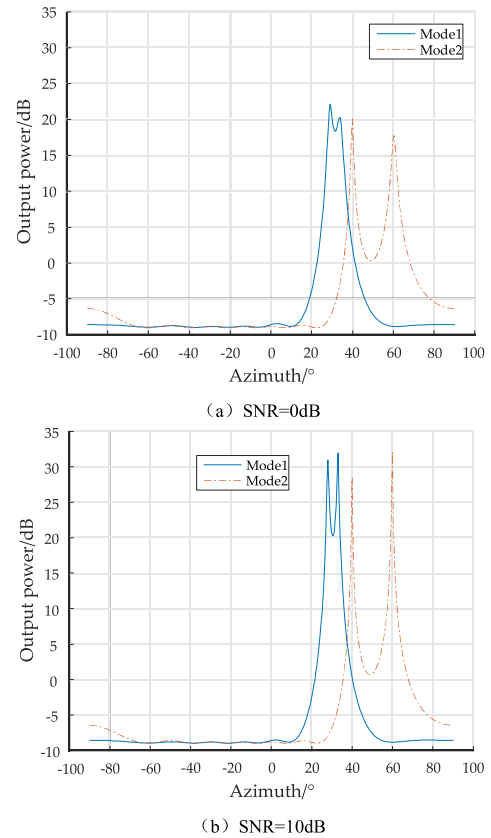

（a）SNR=0dB

（b）SNR=10dB

FIGURE 3. The spectrum peak search diagram of two sources closer and farther apart at different SNRs.

to formula (13), define $P_o = (P(\theta_1) + P(\theta_2))/2$, $\theta_m = (\theta_1 + \theta_2)/2$, $Q(\Delta) = P_o - P(\theta_m)$. When $Q(\Delta) > 0$, $\Delta = |\theta_1 - \theta_2|$ is distinguishable, and its resolution. This part shows the spectral peak search of GA-MUSIC for two sources with different SNRs. If the resolving power condition is satisfied, the solute is considered successful, and the other cases are regarded as unsuccessful.

This part investigates the search capabilities of the GA-MUSIC for signal sources that are closer and farther away through experimentation and analysis. Let the incident angles of the two closer and farther signal sources are 28°, 28° + Δ° (where Δ is 4), and 40°, 60°. The SNR is set to 0dB and 10dB. When the SNR is 0dB, the spectral peak search result of the incident angle 28° and 28° + Δ° is Mode 1. When the incident angle is 40° and 60°, the spectral peak search result is Mode 2. Simulation results are shown in Figure 3a. Similarly, when the SNR is 10 dB, the spectral peak search results at different incident angles are shown in Figure 3b.

Figure 3 shows GA-MUSIC can search the target well regardless of the distance between the two sources. It indicates that GA-MUSIC has good noise immunity.

The following shows the spectral peak search results of GA-MUSIC and PSO-MUSIC at different SNRs. The simulation test $Monte - Carlo$ is set to run 200 times, and the statistical results are shown in Table 1. X in the table represents the number of solutions.

TABLE 1. Number of solutions for two signal sources that are closer and farther apart under different SNRs.

Algorithm	Signal source with close distance				Signal source with far distance			
	X	-10 dB	0dB	5dB	X	-10 dB	0dB	5dB
PSO-MUSIC	0	20	14	7	0	5	3	3
	1	54	45	39	1	14	7	8
	2	126	141	154	2	181	190	189
GA-MUSIC	1	6	1	0	1	0	0	0
	2	194	199	200	200	200	200	200

Table 1 shows the success rate above 97% of spectral peak searches using the GA-MUSIC for sound sources at different SNRs with close distances, and during 200 spectral peak searches, the success rate is 100%. In contrast, the PSO-MUSIC often failed to search the source at close distances. When adjusting the two signal distances to be farther, the search success rate of GA-MUSIC was also significantly higher than that of PSO-MUSIC.

This section investigates the search capabilities of the GA-MUSIC for different SNRs through experimentation and analysis. The results of the GA-MUSIC for various SNRs are shown in Table 2. The error values in the table refer to the maximum and minimum error values ($\Delta_{max}/\Delta_{min}$).

Table 2 shows the optimization performance of the GA-MUSIC is better than that of the PSO-MUSIC when the two signal sources are close to each other. The superiority effect of the GA-MUSIC is more apparent than PSO-MUSIC when the two sources are closer.

When the two peaks are closer, the conventional algorithm will have the problem of premature convergence and incomplete convergence. Furthermore, the GA-MUSIC proposed in this paper can overcome the above defects and have better stability.

In summary, the GA-MUSIC performs is better than the PSO-MUSIC regarding search success rate, number of solutions, and search accuracy. Moreover, the GA-MUSIC has a 100% success rate in finding two sources with good global search performance.

2) THREE SIGNAL SOURCES AT DIFFERENT DISTANCES

This section investigates the search capabilities of the GA-MUSIC for various numbers of signal sources through experimentation and analysis. Parameter setting: set the number of sound sources to 3. The distance between the three signal sources is relatively far as Mode 1. Two of the three signal sources are far apart from the third, and the two signal sources are more relative to each other as Mode 2. The three signal sources are closer to each other as Mode 3. Set the SNR to 10 dB, and the incident angles of the three signal sources in three cases are 20°, 70° and −40°, 28°, 32° and −35°, 40°, 51° and 62°.

Figure 4 shows three signal sources with different distances that can be searched under the GA-MUSIC, which proves
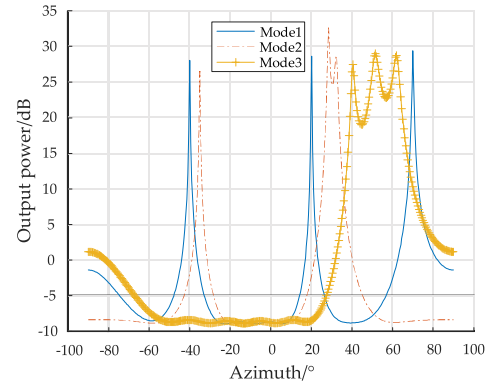

FIGURE 4. Spectral peak diagrams of 3 signal sources when the SNR is 10dB.

that the algorithm has better search performance for multiple signal sources.

Spectrum peak search using GA-MUSIC for the above three operating conditions. The *Monte − Carlo* simulation test is set to run 200 times, and the statistical results are shown in Table 3.

Figure 4 and Table 3 show when the signal sources are at different distances, GA-MUSIC can search the location of three sources. It indicates that GA-MUSIC also has good search performance for multiple sources.

C. ALGORITHM PERFORMANCE ANALYSIS

The array aperture tends to be relatively small due to the size limitation of small underwater platforms. When the array aperture is fixed, the number of array elements is inversely proportional to the array element spacing. According to the theory of array signal processing, theoretically, the more array elements, the better the array orientation effect; the smaller the array element spacing, the better the array orientation effect. However, in actual engineering, the array elements have a certain volume; the array elements have a certain scattering of sound waves. In order to avoid the impact of this scattering on other elements and minimize the acoustic shielding between the elements, the array spacing is generally between 1/10 wavelength to 1/2 wavelength, so in the small aperture platform, the number of sensor array elements can be placed less. Therefore, this paper receive array is a ternary uniform line array, array element spacing $d = 25cm$. Other signal simulation parameters setting as follows: the incident signal is a sinusoidal single source signal, frequency $f_c = 3KHz$, snap number $SNAP$=2048, search angle range $-180° ≤ θ ≤ 180°$. GA-MUSIC simulation parameter settings: population size $Popsize = 90$, crossover probability $P_c = 0.7$, mutation probability parameter $P_m = 0.07$, parameter $γ = 0.1$, phased parameter adjustment $n = 10$, coding length $L = 14$, maximum evolution generation $MaxGen = 200$.

1) ALGORITHM RATE OF SUCCESS COMPARISON

This section uses simulations to verify the success rate for DOA estimation with the same precision and different SNRs

TABLE 2. GA-MUSIC performance of two sound sources closer and farther apart.

SNR/ Error	Two closer-apart sound sources				Two farther-apart sound sources			
	Target 1		Target 2		Target 1		Target 2	
	Error magnitude	Error mean	Error magnitude	Error mean	Error magnitude	Error mean	Error magnitude	Error mean
-10/4°	0.536/0	0.195	0.446/0	0.238	0.139/0	0.097	0.175/0	0.136
0/3°	0.326/0	0.134	0.314/0	0.137	0.133/0	0.104	0.142/0	0.106
5/2°	0.774/0.173	0.143	0.896/0.214	0.152	0.176/0	0.092	0.193/0	0.087

TABLE 3. Number of solutions for two signal sources that are closer and farther apart under different SNRs.

Number of solutions	Mode 1	Mode 2	Mode 3
1	2	5	11
2	19	19	26
3	179	176	163

TABLE 4. Number of solutions for two signal sources that are closer and farther apart under different SNRs.

SNR(dB)	MUSIC	PSO-MUSIC	GA-MUSIC
-15	90.3%	92.3%	95.4%
-10	90.6%	92.6%	95.6%
-5	90.8%	92.9%	95.9%
0	90.9%	93.0%	96.2%
5	91.2%	93.5%	96.5%
10	91.2%	93.5%	96.5%
15	91.2%	93.5%	96.5%
20	91.2%	93.5%	96.5%

TABLE 5. Comparison of the average search time of the three algorithms under different SNRs.

SNR(dB)	MUSIC	PSO-MUSIC	GA-MUSIC
-15	26.5s	25.2s	10.4s
-10	20.4s	19.6s	8.8s
-5	15.6s	15.1s	7.0s
0	12.3s	11.2s	5.2s
5	11.1s	9.6s	2.3s
10	9.8s	7.2s	2.1s
15	7.3s	7.2s	2.1s
20	7.3s	7.2s	2.1s

TABLE 6. Comparison of the average search time of the three algorithms under different SNRs.

Precision(°)	MUSIC	PSO-MUSIC	GA-MUSIC
0.1	20.4s	19.6s	8.8s
1	15.2s	10.3s	5.2s
3	11.6s	8.7s	3.6s

of the proposed GA-MUSIC, including MUISC and PSO-MUSIC adopted as comparison references. The simulation test is set to run 1,000 times. When the difference between the search angles of the three algorithms and the measured incident angles of the sound source target is less than 0.1°, the search is considered successful. The search success rate of the three algorithms is shown in Table 4.

Table 4 shows the search success rate of the MUSIC is between 90.3%~91.2%, the search success rate of the PSO-MUSIC is between 92.3%~93.5%, and the search success rate of the GA-MUSIC is between 95.4%~96.5%. As the SNR increases, the search success rate also increases. When the SNR reaches 5 dB, the search success rates of the three algorithms stabilize and do not change anymore. The GA-MUSIC proposed in this paper has better search performance.

2) ALGORITHM REAL-TIME COMPARISON
The following is to analyze the real-time performance of the MUSIC, PSO-MUSIC, and GA-MUSIC in the search process of DOA estimation peak of signal source under the same accuracy and different SNR conditions simulations are carried out. The simulation test is set to run 1,000 times. When the difference between the search angles of the three

algorithms and the actual incidence angle of the sound source target is less than 0.1°, the search is considered successful. The search time of the three algorithms is recorded 1000 times, and the average value is calculated. The average values of search time for the three algorithms are shown in Table 5.

The following is an analysis of the performance of the MUSIC, PSO-MUSIC, and GA-MUSIC for DOA estimation of signal sources when the SNR is low. The following simulations are performed by adopting the control variable method. The simulation test is set to run 1,000 times. When the SNR is −10 dB, the difference between the search angles of the three algorithms and the actual incident angles of the sound source target is recorded as the search times of 0.1°, 1°, and 3°, respectively, and the mean value is calculated. The mean search time of the three algorithms is shown in Table 6.

From Tables 5 and 6 that when the SNR increases to a certain extent, the spectral peak search process of the MUSIC also takes 7.3 s. In contrast, the PSO-MUSIC has nearly no improvement in real-time performance. Under the premise of ensuring accuracy, the spectral peak search time is almost the same as the MUSIC algorithm, and the real-time performance of the algorithm is not improved. The GA-MUSIC proposed in this paper can search the azimuth information of the sound source target more effectively and quickly when the SNR

is low and has good search performance. When the SNR increases to 10 dB, the GA-MUSIC only needs 2.1 s to search successfully, ensuring the real-time performance of DOA estimation.

3) ALGORITHM COMPARISON

The simulation uses a three-element uniform linear array. The SNR frequency signal $SNR = -10dB$, the number of snapshots $SNAP$=512. The simulation experiment is performed 200 times. The DOA estimation of a single signal source by the MUSIC, PSO-MUSIC, and GA-MUSIC are compared and analyzed. Figures 5a, b, and c show a single signal source's DOA estimation error curve. Other simulation conditions remain unchanged, the SNR is $-10 \sim 25$dB, and the root means the square error is calculated at an equal interval of 2.5dB. The RMSE value between the DOA estimation value and the actual value of the single signal source under different SNRs of the three algorithms is shown in figure 5(d).

Figures 5(a), (b), and (c) show that the estimated value angle error of the MUSIC algorithm is within the range of 2°, the estimated value angle error of the PSO-MUSIC is within 0.5°, and the estimated value angle error of the GA-MUSIC proposed in this paper is within 0.3°. According to the simulated results, the GA-MUSIC proposed in this paper has higher accuracy and better performance in DOA estimation of spectral peak search for single signal sources. As shown in Figure 5(d), the root-mean-square error of all three algorithms keeps decreasing as the SNR increases 0.3 $\sim$ 0.4 the final root-mean-square error converges. Among them, the GA-MUSIC has a faster convergence speed, a smaller minor root mean square error, and better performance.

IV. EXPERIMENTAL RESEARCH

Experimental tests were conducted in an anechoic indoor pool to analyze the feasibility of the GA-MUSIC for engineering applications.

A. EXPERIMENTAL ENVIRONMENT

The experiment's 25m × 12m × 10m indoor anechoic pool has a wedge noise absorber of six-sided anechoic treatment around it. Its effective anechoic frequency is no more than 2 kHz. The upper computer can be used to accurately control the position of an intelligent mechanical motion device that is hung above the pool via a waterproof wire. The transmitting system of the experiment's indoor motion device is mainly composed of a signal generator (Agilent 33522A), a power amplifier (B&K 2713), and a spherical transmitting transducer. The receiving system comprises a vector hydrophone, a programmable filter amplifier PFI28000, a data collector B&K3660D, and a host computer. The vector hydrophone is placed on the bracket of the intelligent mechanical motion device through a retractable elastic device. Three identical transmitting transducers are placed on the same horizontal connection device and assembled with the stand on the smart
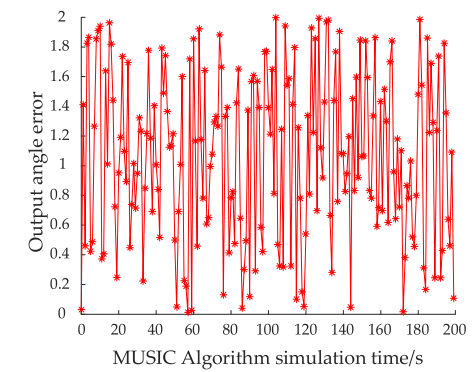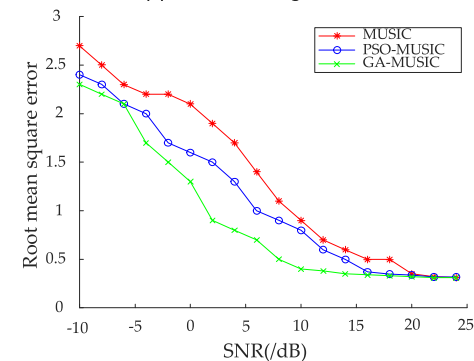

(a) MUSIC Algorithm
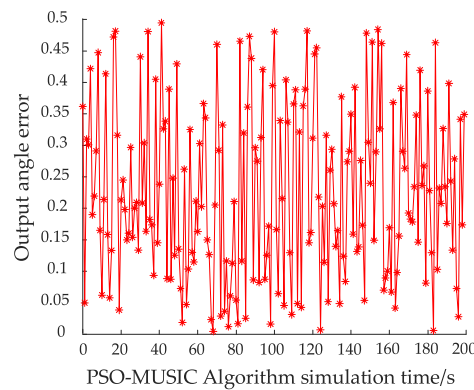
(b) PSO-MUSIC Algorithm
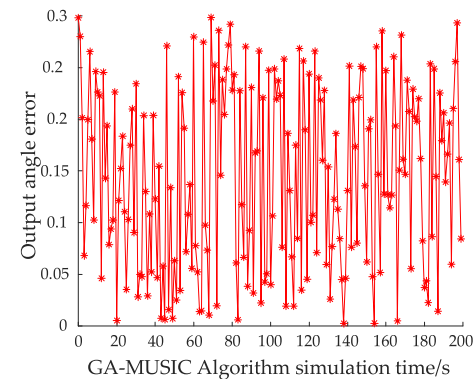
(c) GA-MUSIC Algorithm

(d) Root mean square error diagram under different SNRs

FIGURE 5. The output angle error diagram of the DOA estimation and the three algorithms.
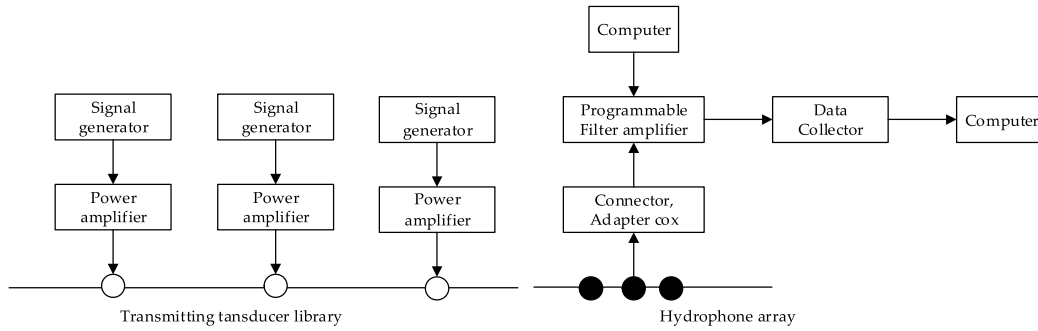
FIGURE 6. Block diagram of experimental instrument connection.

TABLE 7. Comparison of the measured angles of three incoherent sound sources and the calculated angles.

Time(s)	No.1 Source angle (degree)			No.2 Source angle (degree)			No.3 Source angle (degree)		
	Actual	PSO-M	GA-M	Actual	PSO-M	GA-M	Actual	PSO-M	GA-M
0	45.8	46.8	46.0	64.1	65.0	64.0	70.9	71.8	71.1
10	37.3	36.5	37.2	60.9	60.5	61.1	69.1	68.3	69.0
20	25.1	24.3	25.4	56.3	55.9	56.3	66.7	65.8	66.8
30	9.8	10.5	10.0	50.0	48.9	49.8	63.8	62.9	63.9
40	-6.9	-8.1	-7.0	42.3	43.6	42.5	60.0	59.2	59.8
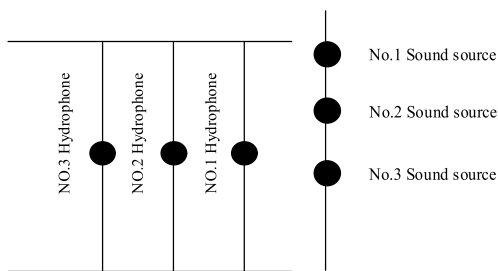
(a) Hydrophone array placement diagram (b) Sound source array placement diagram

FIGURE 7. Diagram of hydrophone and sound source location.

automatic motion device. The transmitting and receiving systems are composed as shown in figure 6.

The hydrophone receives the array, and the sound source signal is laid horizontally in a line array. Firstly, the sensitivity and phase of the hydrophone are corrected by using the calibration data. The theoretical sensitivity value in other directions is calculated based on the axial sensitivity of the x and y channels. The corresponding corrections are made based on the measured sensitivity at different angles. The depth of the transmitting transducer is 4 m, and the sound sources No. 1, No. 2, and No. 3 is arranged at equal intervals at a distance of 1 m. The depth of the hydrophone is 4 m, and the distance between No. 1, No. 2, and No. 3 hydrophones is 0.25 m. The horizontal distance between the hydrophone and the sound source is 20 m. The No. 3 sound source emits a 3 kHz single-frequency signal, and the No. 1 and No. 2 sound sources emit different single-frequency signals. The sampling frequency of the receiving system is 65536 Hz. The position of the sound source and the hydrophone is shown in figure 7.

B. DOA ESTIMATION FOR SINGLE SIGNAL SOURCES

1) RESEARCH ON THE EFFECTIVENESS OF SPECTRAL PEAK SEARCH BY GA-MUSIC FOR SOUND SOURCES WITH SIGNIFICANT FREQUENCY DIFFERENCES

Three incoherent sound sources emit single-frequency sine signals at the same time. The frequencies of sound sources Nos. 1~3 is 5 kHz, 6 kHz, and 3 kHz respectively. The measured signal received by the No. 1 hydrophone is used as a data segment every 10 seconds to calculate the azimuth angle. The spectral peak search angles of the PSO-MUSIC and the GA-MUSIC are recorded in Table 7. In the following table, the PSO-MUSIC is abbreviated as PSO-M, and the GA-MUSIC is abbreviated as GA-M.

Table 7 shows maximum difference between the estimated and measured angles for all three sources under the GA-MUSIC is 0.2°, and the minimum value is 0. The maximum difference values between the estimated and measured angles under the PSO-MUSIC are 1.2°, 1.3°, and 0.9°, and the minimum values are 0.7°, 0.4°, and 0.8°, respectively. The results of the GA-MUSIC in the three cases are fewer errors and better.

2) STUDY ON THE EFFECT OF SPECTRAL PEAK SEARCH BY GA-MUSIC FOR SOUND SOURCES WITH A SLIGHT FREQUENCY DIFFERENCE

Three incoherent sound sources emit single-frequency sine signals at the same time. The frequencies of sound sources Nos. 1–3 are 6 kHz, 6.5 kHz, and 5 kHz, respectively. The measured signal received by the No. 3 hydrophone is used as a data segment every 10 seconds to calculate the azimuth angle. The spectral peak search angles of the PSO-MUSIC and the GA-MUSIC are recorded in Table 8.

TABLE 8. Comparison of the measured angles of three incoherent sound sources and algorithm measured angles.

Time(s)	No.1 Source angle (degree)			No.2 Source angle (degree)			No.3 Source angle (degree)		
	Actual	PSO-M	GA-M	Actual	PSO-M	GA-M	Actual	PSO-M	GA-M
0	45.1	46.5	45.2	-1.5	-2.2	-1.6	-40.4	-41.3	-40.5
10	52.4	51.6	52.4	15.0	16.2	15.1	-29.1	-29.6	-28.9
20	57.9	58.8	58.1	29.4	30.0	29.4	-14.7	-15.1	-14.8
30	62.1	62.8	61.9	40.6	41.2	40.7	1.9	2.3	2.0
40	65.4	66.1	65.5	49.1	48.6	49	18.1	18.6	18.2

Tables 7 and 8 show the GA-MUSIC is more accurate and practical for underwater target orientation estimation than the PSO-MUSIC, which significantly improves the search success rate of underwater target DOA estimation. Moreover, the simulation results of the GA-MUSIC are consistent with the experimental data, which indicates that the algorithm has reference value for practical engineering applications.

V. CONCLUSION

In this paper, an improved GA-MUSIC is proposed through the fusion of the MUSIC algorithm and genetic algorithm, which overcomes the problems of low search success rate and poor real-time performance of the traditional MUSIC algorithm in DOA estimation.

(1) The operator and population improvement optimization strategies are proposed for the defects of the genetic algorithm, such as convergence and the tendency to fall into local optimal solutions. It is shown that the improved genetic algorithm can effectively improve population diversity and search ability and solve the problems of the population being prone to premature maturity and falling into local optimal solutions.

(2) The simulation is based on the GA-MUSIC and the traditional MUSIC algorithm, and the performance of the DOA estimation of signal sources is compared and analyzed. It is shown that the GA-MUSIC works best with different accuracy and SNRs. The GA-MUSIC has a higher search success rate, requires less computing time, and provides better real-time performance.

(3) For practical engineering applications of incoherent multi-source DOA estimation, the GA-MUSIC can effectively improve the search success rate and ensure the accuracy of the output orientation angle of the underwater target. The simulation test of the GA-MUSIC is consistent with the experimental results and can effectively solve the problems of practical engineering applications.

REFERENCES

[1] H. Park and J. Li, "Efficient sparse parameter estimation based methods for two-dimensional DOA estimation of coherent signals," *IET Signal Process.*, vol. 14, no. 9, pp. 643–651, Oct. 2020, doi: 10.1049/iet-spr.2020.0201.

[2] B. Sun, C. Wu, H. Ruan, W. Ye, and T. Su, "High accuracy DOA estimation method with array sensor failure," *Acta Electron. Sinica*, vol. 48, no. 9, pp. 1688–1694, Sep. 2020.

[3] W. Wang, M. Z. B. Yao, Q. Yin, and P. Mu, "Computationally efficient direction-of-arrival estimation of non-circular signal based on subspace rotation technique," *J. Commun.*, vol. 41, no. 11, pp. 198–205, Dec. 2020.

[4] W. Wang, Q. Zhang, W. Shi, W. Tan, and X. Wang, "DOA estimation of vector sensor arrays based on sparse signal power iterative compensation," *J. Vib. Shock*, vol. 39, no. 15, pp. 48–57, Jul. 2020.

[5] S. V. R. Rao, A. M. Prasad, and C. S. Rani, "A HGGSA approach to beam forming for DOA estimation in smart antenna arrays," *Wireless Pers. Commun.*, vol. 115, no. 3, pp. 2391–2413, Aug. 2020.

[6] J. Li, X. Gu, R. Zhan, X. Xiong, and Y. Liu, "DOA estimation without source number for cyber-physical interactions," *Complexity*, vol. 2020, pp. 1–5, Jul. 2020, doi: 10.1155/2020/9768361.

[7] Y. Xie, M. Huang, Y. Zhang, T. Duan, and C. Wang, "Two-stage fast DOA estimation based on directional antennas in conformal uniform circular array," *Sensors*, vol. 21, no. 1, p. 276, Jan. 2021.

[8] J. Li, Q.-H. Lin, C.-Y. Kang, K. Wang, and X.-T. Yang, "DOA estimation for underwater wideband weak targets based on coherent signal subspace and compressed sensing," *Sensors*, vol. 18, no. 3, p. 902, Mar. 2018.

[9] S. Wei, Y. Long, R. Liu, and Y. Su, "A two-step compressed sensing approach for single-snapshot DOA estimation of closely spaced signals," *Math. Problems Eng.*, vol. 2021, pp. 1–11, Feb. 2021.

[10] A. Fisne, B. Kilic, A. Güngör, and A. Ozsoy, "Efficient heterogeneous parallel programming for compressed sensing based direction of arrival estimation," *Concurrency Comput., Pract. Exp.*, vol. 34, no. 9, Apr. 2022, Art. no. e6490.

[11] H. Yan, T. Chen, P. Wang, L. Zhang, R. Cheng, and Y. Bai, "A direction-of-arrival estimation algorithm based on compressed sensing and density-based spatial clustering and its application in signal processing of MEMS vector hydrophone," *Sensors*, vol. 21, no. 6, p. 2191, Mar. 2021.

[12] B. Hu, X. Shen, M. Jiang, and K. Zhao, "Off-grid DOA estimation based on compressed sensing on multipath environment," *Int. J. Antennas Propag.*, vol. 2023, pp. 1–6, Apr. 2023.

[13] J. Ma, J. Zhang, Z. Yang, and T. Qiu, "Off-grid DOA estimation using sparse Bayesian learning for MIMO radar under impulsive noise," *Sensors*, vol. 22, no. 16, p. 6268, Aug. 2022.

[14] J. Yuan, G. Zhang, H. Leung, and S. Ma, "Off-grid DOA estimation for noncircular signals via block sparse representation using extended transformed nested array," *IEEE Signal Process. Lett.*, vol. 30, pp. 130–134, 2023.

[15] J. Chouragade and R. K. Muthu, "Continuous mapping of broadband VHF lightning sources by real-valued MUSIC," *IEEE Trans. Geosci. Remote Sens.*, vol. 60, 2022, Art. no. 4102707.

[16] N. Ahmed, H. Wang, M. A. Z. Raja, W. Ali, F. Zaman, W. U. Khan, and Y. He, "Performance analysis of efficient computing techniques for direction of arrival estimation of underwater multi targets," *IEEE Access*, vol. 9, pp. 33284–33298, 2021.

[17] H. Dou, F. Yang, Z. Xiao, and L. Sun, "Two-dimensional MUSIC spectral peak search algorithm based on chicken swarm optimization," *J. Beijing Inst. Technol.*, vol. 44, no. 11, pp. 32–40, Nov. 2022.

[18] R. Li, J. Zhang, M. Bao, X. Hu, L. Guan, and Y. Xu, "Direction of arrival estimation of signals using wavelet transform," *Acta Acustica*, vol. 44, no. 1, pp. 77–85, Jan. 2019.

[19] Y. Guo and C. Wang, "Research on MUSIC-DOA estimation method based on SVM steered response power," *J. Nanjing Univ. Sci. Technol.*, vol. 43, no. 2, pp. 237–243, May 2019.

[20] M. Jia, Y. Jia, S. Gao, J. Wang, and S. Wang, "Multi-source DOA estimation in reverberant environments using potential single-source points enhancement," *Appl. Acoust.*, vol. 174, Mar. 2021, Art. no. 107782.

[21] Z. Zheng, Y. Huang, W. Wang, and H. C. So, "Direction-of-arrival estimation of coherent signals via coprime array interpolation," *IEEE Signal Process. Lett.*, vol. 27, pp. 585–589, Mar. 2020, doi: 10.1109/LSP.2020.2982769.

[22] V.-S. Doan and D.-S. Kim, "DOA estimation of multiple non-coherent and coherent signals using element transposition of covariance matrix," *ICT Exp.*, vol. 6, no. 2, pp. 67–75, Jun. 2020.

[23] H. Xu, D. Wang, B. Ba, W. Cui, and Y. Zhang, "Direction-of-arrival estimation for both uncorrelated and coherent signals in coprime array," *IEEE Access*, vol. 7, pp. 18590–18600, 2019.

[24] R. Suleesathira, "Direction of arrival identification using MUSIC method and NLMS beamforming," in *Proc. 15th Int. Joint Symp. Artif. Intell. Natural Lang. Process. (iSAI-NLP)*, Bangkok, Thailand, Nov. 2020, pp. 1–6.

[25] M. Shi, "A polarization sensitive DOA estimation algorithm based on rotating array," *Commun. Technol.*, vol. 53, no. 12, pp. 2927–2935, Dec. 2020.

[26] P. Wang, F. He, F. Zhang, and Y. Bai, "Maximum likelihood DOA estimation based on artificial fish swarm algorithms for acoustic vector sensor array," *J. Taiyuan Univ. Technol.*, vol. 51, no. 6, pp. 845–851, Nov. 2020.

[27] T. Li, P. Han, G. Zhou, and X. Yao, "A joint processing-music algorithm in multipath environment based on non-uniform line array," in *Proc. 13th Int. Congr. Image Signal Process., Biomed. Eng. Informat. (CISP-BMEI)*, Chengdu, China, Oct. 2020, pp. 495–500.

[28] J. Zhao, R. Gui, and X. Dong, "PHD filtering for multi-source DOA tracking with extended co-prime array: An improved MUSIC pseudo-likelihood," *IEEE Commun. Lett.*, vol. 25, no. 10, pp. 3267–3271, Oct. 2021.

[29] A. Liu, D. Yang, S. Shi, Z. Zhu, and Y. Li, "Augmented subspace MUSIC method for DOA estimation using acoustic vector sensor array," *IET Radar, Sonar Navigat.*, vol. 13, no. 6, pp. 969–975, Jun. 2019.

[30] D. Meng, X. Wang, M. Huang, L. Wan, and B. Zhang, "Robust weighted subspace fitting for DOA estimation via block sparse recovery," *IEEE Commun. Lett.*, vol. 24, no. 3, pp. 563–567, Mar. 2020.

[31] J.-C. Hung and A.-C. Chang, "Combining genetic algorithm and iterative MUSIC searching DOA estimation for the CDMA system," *Expert Syst. Appl.*, vol. 38, no. 3, pp. 1895–1902, Mar. 2011.

HUAN CHEN received the Ph.D. degree from Harbin Engineering University, Harbin, China, in 2011.

He is currently working at the China Ship Development and Design Center, Wuhan, China. His current research interests include target location and recognition and noise control technology.

LEI ZHANG is currently the Deputy Director with the Hospital of Beidahuang Industry Group General. His current research interests include intelligent healthcare, bio-information processing and modeling, and deep learning.

RUI GUO is currently pursuing the Ph.D. degree with the Harbin University of Science and Technology. Her main research interests include target location and recognition and noise control technology.

CHUANG HAN received the Ph.D. degree from Harbin Engineering University, Harbin, China, in 2015.

His current research interests include target location and recognition and noise control technology.

CHAOFENG LAN received the Ph.D. degree from Harbin Engineering University, Harbin, China, in 2012.

She was a Postdoctoral Fellow with the Harbin Institute of Technology, Harbin, in 2018. She is currently an Associate Professor with the Harbin University of Science and Technology. She has authored or coauthored more than 30 refereed publications and presided over one NSFC, two provincial, one bureau level project, one university open project, and one university-enterprise cooperation project. Her current research interests include intelligent speech interaction, image processing, target location and recognition, and noise control technology.

DAJUN LUO is currently pursuing the master's degree. His main research interests include noise control technology and deep learning.

• • •